# Size effect on the dielectric properties of $BaTiO_3$ nanoceramics in a modified Ginsburg-Landau-Devonshire thermodynamic theory

Shan Lin,[1,2] Tianquan Lü,[2] Changqing Jin,[1,*] and Xiaohui Wang[3]
[1]*Laboratory for Condensed Matter Physics, Institute of Physics, Chinese Academy of Sciences, Beijing 100080, Peoples Republic of China*
[2]*Department of Physics, Jilin University, Changchun, China*
[3]*Department of Materials Sciences, Tsinghua University, Beijing, China*
(Received 2 May 2006; revised manuscript received 24 July 2006; published 30 October 2006)

Grain size effects on the dielectric properties of $BaTiO_3$ nanoceramics have been studied by using the modified Ginsburg-Landau-Devonshire (GLD) thermodynamic theory. Considering the existence of internal stresses, it is found that with decreasing grain size the transition temperature of cubic-tetragonal phase decreases, while those of tetragonal-orthorhombic and orthorhombic-rhombohedral phases increase. With further reducing grain size, our model predicts that the two ferroelectric structures of orthorhombic and tetragonal phases will become unstable and disappear at a critical size, leaving only one stable ferroelectric phase of rhombohedral structure. Consequently, a theoretical phase diagram of the transition temperature versus grain size is established wherein two triple points and a reentrance behavior are indicated. The results are compared with experimental data.

DOI: 10.1103/PhysRevB.74.134115 PACS number(s): 64.70.−p, 77.84.−s, 81.07.−b

## I. INTRODUCTION

Since the birth of ferroelectric $BaTiO_3$ (BT) ceramics in the early 1940s, they have attracted great interest due to their excellent properties. In recent years, ferroelectric ceramics have been widely employed in the modern microelectronic industry for applications including multilayer ceramics capacitors, ferroelectric memories, and piezoelectric transducers.[1] The importance of grain size effects is apparent, especially when considering the miniaturization requirement of the microelectronics industry.

It is well known that BT single crystals undergo some phase transitions from cubic to tetragonal (C-T), tetragonal to orthorhombic (T-O), and orthorhombic to rhombohedral (O-R) with decreasing temperature. When scaled down to the submicrometer-scale or nanoscale dimensions, BT materials will exhibit some different properties. Various experimental techniques were used to study the crystal structure and phase transition of BT, and corresponding theoretical investigations were carried out in many works.[2–10] Early experimental works showed that a critical size existed in the particle and the thin film below which the ferroelectricity would disappear. Uchino *et al.*[2] found that the critical size of a BT particle was about 120 nm at room temperature. W. L. Zhong[3] predicted the critical thickness of a BT film to be 38 nm. Recently, it has been reported that the critical size should be much smaller for both the BT particle (16 nm[4] or 30 nm[5]) and the BT thin film (2.4 nm[6] or 5 nm[7]).

In ceramics materials, since individual crystallites are surrounded by grain boundaries, the mechanical effect caused by the elastic three-dimensional clamping of crystallite may play an important role in shaping the overall performance. Actually, the internal stress caused by the phase transition can be relieved by formation of 90° domains, so the contribution of the 90° domain walls to the dielectric constant is dominating in coarse-grained ceramics.[11–13] With further decreasing grain size, the single domain becomes energetically favorable. Consequently, in fine-grained ceramics, the contribution of the stress should be taken into account due to the absence of 90° domains. It is for this reason that the dielectric constant of fine-grained BT ceramics has a maximum at about $0.7 \sim 1.0$ $\mu$m and then decreases strongly with further reducing grain size.[12,13] Shaikh reported this maximum at about 0.4 $\mu$m.[14]

Here we discuss only the dielectric properties of the nanoceramics. It can therefore be assumed that the grain is single domain and that only the grain boundary and stress contributions to the dielectric constant should be considered. The grain boundary is thought to have a lower dielectric constant than the ferroelectric grain, since with decreasing grain size, the fraction of grain boundary volume increases and the corresponding ceramics dielectric constant is reduced.[14–16] By measuring the dielectric constant versus temperature for small-scale ceramics, it was shown that the transition temperature of cubic-tetragonal phase ($T_{C\text{-}T}$) decreased while those of tetragonal-orthorhombic ($T_{T\text{-}O}$) and orthorhombic-rhombohedral ($T_{O\text{-}R}$) increased with reducing grain size.[12,13,17–20] At room temperature, the coexistence of the tetragonal and orthorhombic phases was observed in fine-grained ceramics,[12,19–21] and the population of the orthorhombic phase increased with further decreasing grain size.[12,19,22] Many authors attributed these changes of structures and transition temperatures to the effect of the internal stress. Experimentally, Samara[23] reported that the Curie temperature of pure BT ceramics decreased linearly with increasing hydrostatic pressure, and that the corresponding transition peak value was suppressed. For the BT single crystal, the three transition temperatures, $T_{C\text{-}T}$, $T_{T\text{-}O}$, and $T_{O\text{-}R}$, were observed to shift to lower temperatures under hydrostatic pressure.[24] Theoretically, Buessem *et al.*[25]simulated the effect of a three-dimensional stress on the dielectric constant, but they only described BT ceramics with the tetragonal structure. Using a nonlinear thermodynamics theory, Zembilgotov *et al.*[26] calculated $T_{O\text{-}R}$ of BT nanoceramics and

 

found that it can increase to 19 °C, whereas it is −71 °C in BT single crystals. Moreover, a mixture of the rhombohedral and orthorhombic phases was predicted to occur at temperature range of 19 to 55 °C for the BT nanoceramics; however, they did not show the relationship between the overall shifts of the three transition temperatures ($T_{R\text{-}O}$, $T_{O\text{-}T}$, $T_{T\text{-}C}$) and grain size.

The phenomenological Ginsburg-Landau-Devonshire (GLD) theory is an efficient approach to studying the properties of the BT single crystals,[27,28] thin films,[3,29] and the particles.[30,31] Due to the fact that the mechanical boundary conditions of the single crystal and isolated particles are really different from those of grains in a dense ceramic, a new GLD free energy potential should be constructed to investigate size effects on the dielectric properties of these systems.

In this paper, considering the combined effects of the stresses and grain size, we assume that some GLD free energy coefficients depend on grain size and can be written as functions of grain size. So a new GLD free energy with modified coefficients can be proposed to explain the size-driven phase transitions in nanoceramics. The properties of dense nanoceramics such as the dielectric constant, phase transition temperature, and the critical size can be successfully described by this model and are in good agreement with experimental data. Furthermore, a theoretical phase diagram of tens of nanometers grain size ceramics is predicted which shows novel critical phenomena with two triple points and a reentrance behavior as a function of grain size.

## II. PHENOMENOLOGICAL SIZE EFFECT MODEL FOR FERROELECTRIC CERAMICS

We assume that the grain in dense nanoceramics is single domain. Using the GLD formalism, the elastic Gibbs free energy is expanded as a polynomial of the polarization components $P_i(i=1,2,3)$. Considering the effect of mechanical stress, the elastic Gibbs free energy function can be written as[27,28,32]

$$
\begin{aligned}
G_1 &= \alpha_1(T)(P_1^2+P_2^2+P_3^2)+\alpha_{11}(P_1^4+P_2^4+P_3^4)\\
&+\alpha_{12}(P_1^2P_2^2+P_2^2P_3^2+P_3^2P_1^2)+\alpha_{111}(P_1^6+P_2^6+P_3^6)\\
&+\alpha_{112}[P_1^2(P_2^4+P_3^4)+P_2^2(P_1^4+P_3^4)+P_3^2(P_1^4+P_2^4)]\\
&+\alpha_{123}P_1^2P_2^2P_3^2+\alpha_{1111}(P_1^8+P_2^8+P_3^8)\\
&+\alpha_{1112}[P_1^6(P_2^2+P_3^2)+P_2^6(P_1^2+P_3^2)+P_3^6(P_1^2+P_2^2)]\\
&+\alpha_{1122}(P_1^4P_2^4+P_2^4P_3^4+P_1^4P_3^4)\\
&+\alpha_{1123}(P_1^4P_2^2P_3^2+P_2^4P_1^2P_3^2+P_3^4P_1^2P_2^2)\\
&-\frac{1}{2}S_{11}(\sigma_1+\sigma_2^2+\sigma_3^2)-S_{12}(\sigma_1\sigma_2+\sigma_2\sigma_3+\sigma_1\sigma_3)\\
&-\frac{1}{2}S_{44}(\sigma_4^2+\sigma_5^2+\sigma_6^2)-Q_{11}(\sigma_1P_1^2+\sigma_2P_2^2+\sigma_3P_3^2)\\
&-Q_{12}[\sigma_1(P_2^2+P_3^2)+\sigma_2(P_1^2+P_3^2)+\sigma_3(P_1^2+P_2^2)]\\
&-Q_{44}(P_2P_3\sigma_4+P_1P_3\sigma_5+P_2P_1\sigma_6) \qquad (1)
\end{aligned}
$$

Here $P_i$ is the polarization; $\sigma_i$ are stress components in Voigt notation; $\alpha_i$, $\alpha_{ij}$, $\alpha_{ijk}$, and $\alpha_{ijkl}$ are the dielectric stiffness and higher-order stiffness coefficients at constant stress; $S_{ij}$ is the elastic compliance coefficients at constant polarization; and $Q_{ij}$ is the cubic electrostrictive constant. It was found that Landau coefficients up to the sixth order were not considerable enough to account for the phase transitions under larger compressive strains, so it become necessary to include higher orders.[8] Here we use the parameters[33] of the elastic Gibbs function, which were taken from Refs. 28 and 29.

To determine the equilibrium thermodynamic states of the BT single crystal, one should calculate all of the minima of $G_1$ with respect to the components of the polarization and then select the phase which corresponds to the minimum. It can be found that there are four possible phases in the bulk material corresponding to the cubic, tetragonal, orthorhombic, and rhombohedral structures, respectively: (1) the cubic phase: $P_1^2=P_2^2=P_3^2=0$; (2) the tetragonal phase: $P_1^2=P_2^2=0, P_3^2\neq 0$; (3) the orthorhombic phase: $P_1^2=P_3^2\neq 0$, $P_2^2=0$; and (4) the rhombohedral phase: $P_1^2=P_2^2=P_3^2\neq 0$. Here, for simplicity, we describe the contribution of the hydrostatic pressure and the shear stress with $\sigma_1=\sigma_2=\sigma_3<0$ and $\sigma_4=\sigma_5=\sigma_6>0$, respectively.

Based on Eq. (1), the hydrostatic pressure can renormalize the coefficient $\alpha_1(T)$ of the second-order polarization terms and ultimately shifts the Curie temperature to lower temperature linearly.[34,35] Actually, it was experimentally reported that the surface tension effect can be assimilated to the application of a hydrostatic pressure,[2] and this hydrostatic pressure $P$ and the variation of Curie temperature $T_C$, can be written as $1/R$ and $-1/R$, respectively, where $R$ is the radius of the particle.[2] That is, the Curie temperature will decrease with reducing the grain size due to the existence of the hydrostatic pressure.

The contribution of shear stress cannot be ignored in dense nanoceramics. It is reported that the shear stress may be plays the possible role in enhancing the stability of the orthorhombic structure within the grains of polycrystalline $BaTiO_3$.[11,12,19] Since the unit cell of orthorhombic $BaTiO_3$ is characterized by a shear deformation of the cubic perovskite cell, it is understandable that $BaTiO_3$ would do so to some extent when under the influence of increasing shear stresses. Based on the observed experimental phenomena, it seems that contribution of the shear stress may increase with decreasing grain size, and the increase of shear stresses favors the stabilization of the R and O phases, and makes corresponding transition temperatures $T_{R\text{-}O}$ and $T_{O\text{-}T}$ move to higher temperatures.

Based on the discussion above, considering the influence of the stresses on the charge tendency of free energy and the relationship between the stresses and grain size, the coefficients $\alpha_1(T)$ and $\alpha_{12}$ can then be written as the function of grain size $\alpha_1^*(T,d)$ and $\alpha_{12}^*(d)$, respectively. A new GLD free energy can be described as follows:

$$
\begin{aligned}
\tilde{G}_1 &= \alpha_1^*(T,d)(P_1^2+P_2^2+P_3^2)+\alpha_{11}(P_1^4+P_2^4+P_3^4)\\
&+\alpha_{12}^*(d)(P_1^2P_2^2+P_2^2P_3^2+P_3^2P_1^2)+\alpha_{111}(P_1^6+P_2^6+P_3^6)\\
&+\alpha_{112}[P_1^2(P_2^4+P_3^4)+P_2^2(P_1^4+P_3^4)+P_3^2(P_1^4+P_2^4)]
\end{aligned}
$$

$$+ \alpha_{123}P_1^2P_2^2P_3^2 + \alpha_{1111}(P_1^8 + P_2^8 + P_3^8)$$
$$+ \alpha_{1112}[P_1^6(P_2^2 + P_3^2) + P_2^6(P_1^2 + P_3^2) + P_3^6(P_1^2 + P_2^2)]$$
$$+ \alpha_{1122}(P_1^4P_2^4 + P_2^4P_3^4 + P_1^4P_3^4)$$
$$+ \alpha_{1123}(P_1^4P_2^2P_3^2 + P_2^4P_1^2P_3^2 + P_3^4P_1^2P_2^2) \quad (2)$$

$$\alpha_1^*(T,d) = \alpha_1(T) + \frac{K_1}{d}$$

$$\alpha_{12}^*(d) = \alpha_{12} + \frac{K_2}{d}. \quad (3)$$

Here parameter $d$ is the ceramics grain size in meters, and the coefficients $\alpha_1^*(T,d)$ and $\alpha_{12}^*(d)$ are size dependent. Taking into account experimental results, we choose $K_1 = 0.46\ \mathrm{Jm^2/C^2}$ and $K_2 = -10.0\ \mathrm{Jm^6/C^4}$. When $d$ is close to infinity, Eq. (2) describes the properties of the single crystal, and the corresponding transition temperatures $T_{C\text{-}T}$, $T_{T\text{-}O}$, and $T_{O\text{-}R}$ are 125 °C, 8 °C, and −71 °C, respectively.[28]

The reciprocal dielectric susceptibilities $\eta_{ij}$ can be obtained from appropriate second-partial derivatives of Eq. (2); the corresponding dielectric susceptibilities $\chi_{ij}$ can then be written as

$$\eta_{ij} = \epsilon_0 \frac{\delta^2 \tilde{G}_1}{\delta P_i \delta P_j} \quad \text{and} \quad \chi_{ij} = \frac{(-1)^{i+j} A_{ij}}{\Delta} \quad (4)$$

Here, $\Delta$ is the determinant of the $\eta_{ij}$ matrix and $A_{ij}$ is the cofactor of $\eta_{ij}$. The dielectric constant tensor for a ceramics grain can be written as a diagonalization matrix:

$$\begin{pmatrix} \chi_{11} & \chi_{12} & \chi_{13} \\ \chi_{21} & \chi_{22} & \chi_{23} \\ \chi_{31} & \chi_{32} & \chi_{33} \end{pmatrix} \Rightarrow \begin{pmatrix} \chi'_{11} & 0 & 0 \\ 0 & \chi'_{22} & 0 \\ 0 & 0 & \chi'_{33} \end{pmatrix}. \quad (5)$$

Since the ceramics dielectric susceptibility is isotropic while each individual ferroelectric crystallite is anisotropic, we should get the average susceptibility of ceramics by transformation of coordinates. Two Cartesian coordinate systems are introduced: the ceramics system $(x,y,z)$ and the crystallographic coordinate system $(x',y',z')$. Two systems are related by Euler's angles $\varphi$, $\psi$, and $\theta$, and assuming all lattice orientations of crystallites in the paraelectric state are equally probable, the average dielectric susceptibility can be obtained as follows:[26]

$$\bar{\chi}_{ij} = \frac{1}{8\pi^2} \int_0^{2\pi} d\varphi \int_0^{2\pi} d\psi \int_0^{\pi} \chi_{ij}(\varphi,\psi,\theta) \sin\theta d\theta. \quad (6)$$

We can get the average dielectric susceptibility from Eq. (6),

$$\bar{\chi} = \frac{1}{3}(\chi'_{11} + \chi'_{22} + \chi'_{33}) \quad (7)$$

Here, $\chi'_{11}, \chi'_{22}$, and $\chi'_{33}$ are the dielectric constant tensor for the ceramics grain, as shown in Eq. (5).

Considering the effect of grain boundary, which has a low-permittivity $\varepsilon_d$ and an effective thickness $l$, the total dielectric susceptibility $\varepsilon$ can be evaluated as[15]

$$\epsilon \approx \frac{3\epsilon_d(\epsilon_g + 2\epsilon_d)}{\epsilon_g + 2\epsilon_d - (\epsilon_g - \epsilon_d)\left(\frac{d}{d+2l}\right)} - 2\epsilon_d$$

$$\epsilon_g = \bar{\chi} + 1. \quad (8)$$

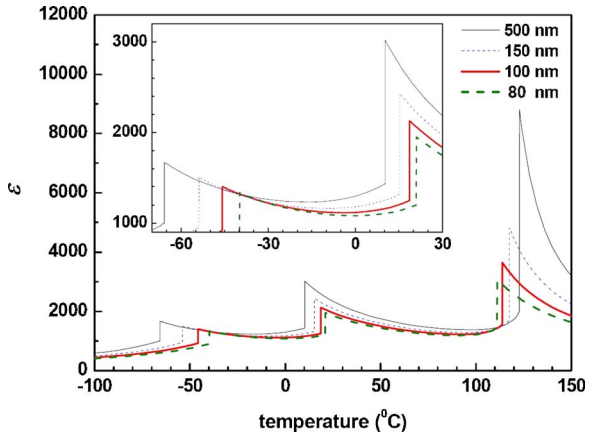


FIG. 1. (Color online) The total dielectric constant $\varepsilon$ as a function of temperature with different grain size. Inset: A close-up of the lower temperature region.

The effect of grain size on BT ceramics properties (such as dielectric constant, phase transition temperature, etc.) can be studied using Eqs. (2)–(8).

## III. RESULTS AND DISCUSSION

The temperature dependence on the total dielectric constant with different grain size is shown in Fig. 1. A close-up of the lower temperature is shown in the inset. Grain sizes are $d$=500, 150, 100, and 80 nm, respectively, and $\varepsilon_d$=70, $l$=0.7 nm. It is found that there are three dielectric peaks, which represent three phase transitions of R-O, O-T, and T-C, respectively. With decreasing $d$, the two lower dielectric peaks (i.e., R-O and O-T) move to higher temperatures; however, the T-C dielectric peak moves to lower temperature. Furthermore, the corresponding values of all the dielectric peaks are depressed when grain size decreases. These results agree very well qualitatively with the experimentally measured results for BT nanoceramics,[13,18,19,36] but there are some quantitative differences. Our results show the dielectric peaks are still sharp with decreasing grain size, yet experimentally measured dielectric peaks are obviously broad and diffuse with decreasing grain size, also the corresponding values are strongly depressed. These quantitative differences are a result of our assumptions that the hydrostatic pressure and the shear stresses are homogenous and that grain size is uniform in dense nanoceramics. In reality, the stresses between grains are very complex and there is a significant grain size distribution in dense nanoceramics. It is therefore necessary to account for nonuniform distribution of grain

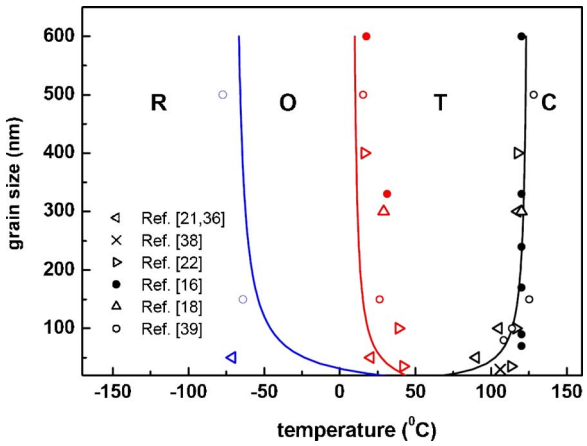


FIG. 2. (Color online) The three transition temperatures $T_{R\text{-}O}$, $T_{O\text{-}T}$, $T_{T\text{-}C}$ dependence of grain size. Experimental data are taken from Refs. 16, 18, 21, 22, 36, 38, and 39, respectively. The crystal structure of a nanocrystalline BT ceramic is denoted by C(cubic), T(tetragonal), O(orthorhombic), and R(rhombohedral).

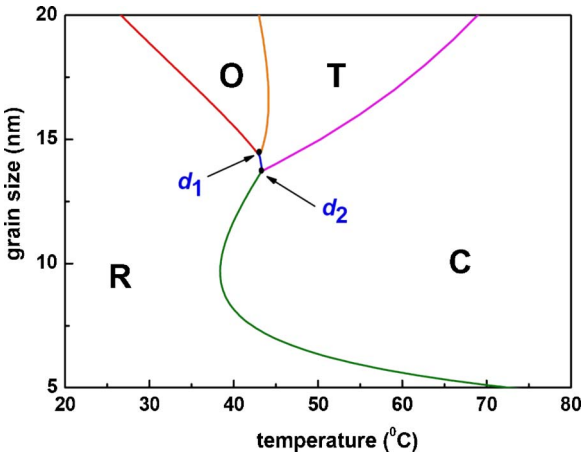


FIG. 3. (Color online) Phase diagram of the transition temperature versus grain size. Two triple points are marked with $d_1$ and $d_2$. The reentrance behavior from R to C and then to R is observed as a function of grain size.

sizes[10,31] and gradients of the stress[37] to explain these quantitative differences.

Figure 2 shows the transition temperatures dependence of the grain size. The solid lines are our theoretical results, and the symbol points represent experimental data taken from Refs. 16, 18, 21, 22, 36, 38, and 39, respectively. Here the grain size range is from 20 nm to 600 nm. The transition temperatures of ceramic with grain size below 20 nm are shown in Fig. 3. The results indicate that with decreasing grain size $T_{R\text{-}O}$ and $T_{O\text{-}T}$ increase, while $T_{T\text{-}C}$ decreases. Furthermore, $T_{R\text{-}O}$ and $T_{O\text{-}T}$ are more effectively influenced by the grain size than $T_{T\text{-}C}$. It is also found that: (1) when the grain size is fixed, all the phase transitions from R to O, O to T, and T to C will occur with increasing temperature; (2) when temperature is fixed, the size-driven phase transition will take place. For example, at room temperature, the tetragonal phase is stable in large-scale ceramics, while with decreasing grain size, the structure will change from T to O, and then from O to R. This result is in accord with experimental data. To date, published studies have predominantly focused on the phase transition at room temperature, or on the ferroelectric to paraelectric transition. Consequently, experimental data for $T_{R\text{-}O}$ are much more rare than data concerning $T_{O\text{-}R}$ and $T_{T\text{-}C}$. In addition, the observed x-ray peaks for smaller grain sizes are broad, and the dielectric peaks for these reduced grain sizes are depressed and diffuse. Furthermore, the observed Raman spectra show that the phase transition takes place over a large range of temperatures in which these phases might coexist. Given the difficulty in obtaining the exact phase transition temperature and grain size in dense nanoceramics, we believe that our data is in good agreement with experimental data, despite the slight differences.

At present, the smallest grain size reported in the literatures for dense BT nanoceramics is about 20 nm.[20] Our model allows one to predict the phase transition properties in a few tens of nanometers or even a few nanometers grain size ceramics, but it is really difficult to prepare the sample with a nanometer grain size and figure out the properties of phase transition in experiments at the moment. A phase diagram of the transition temperature versus grain size is shown in Fig. 3. There are two predicted triple points, and the corresponding sizes are marked $d_1$ and $d_2$. One triple point is at critical grain size $d_1$ for O, T, and R phase, respectively. The other triple point is at critical grain size $d_2$ for T, C, and R, respectively. The results indicate that the O phase and T phase become unstable and disappear as grain size shrinks to $d_1$ and $d_2$ respectively, meaning that $d_1$ and $d_2$ are critical sizes for the O phase and T phase. With further decreasing grain size, the only stable ferroelectric structure is rhombohedral. In addition, an interesting phenomenon can be observed by using our model, that is, variations of $T_{O\text{-}T}$ and $T_{R\text{-}C}$ with decreasing grain size are not monotonous near the two triple points. This kind of size-derived reentrance is probably caused by the competition between the hydrostatic pressure and the shear stress. It is understandable that the hydrostatic pressure favors stabilization of the cubic structure; however, the shear stress is in favor of the existence of the rhombohedral structure. The predicated two triple critical points as well as the reentrance behavior of BT at certain critical grain sizes might be realized experimentally through sophistically tuning grain size and shear strain in ultrathin films.

## IV. CONCLUSIONS

Using a modified GLD thermodynamic theory, the grain size effect on the dielectric properties of nanoscale ceramics is investigated by taking the existence of the internal stresses into account. The results show that with reducing grain size, ferroelectric-ferroelectric transition temperatures $T_{R\text{-}O}$ and $T_{O\text{-}T}$ become higher, while the ferroelectric-paraelectric transition temperature $T_{T\text{-}C}$ becomes lower. The dielectric constants are depressed by considering the effect of grain boundary. It is predicted that the O and T ferroelectric phases are unstable and disappear at the certain critical size, respectively, and that only the R structure is stable in small dense

ceramics, characterized with two triple critical points around the critical size. In addition, the transition temperature from R to C varies nonmonotonously with further decreasing grain size, accompanied by a reentrance behavior.

**ACKNOWLEDGMENTS**

This work was supported by Ministry of Science and Technology and NSF of China through research projects 2002CB613301, 90401003, and 50332020.

*Corresponding author. Email: Jin@aphy.iphy.ac.cn

[1] Gene H. Haertling, J. Am. Ceram. Soc. **82**, 797 (1999).
[2] Kenji Uchino, Eiji Sadanaga, and Terukiyo Hirose, J. Am. Ceram. Soc. **72**, 1555 (1989).
[3] W. L. Zhong, Y. G. Wang, and P. L. Zhang, Phys. Lett. A **189**, 121 (1994).
[4] S. Aoyagi, Y. Kuroiwa, A. Sawada, H. Kawaji, and T. Atake, J. Therm Anal. Calorim. **81**, 627 (2005).
[5] Fu-Su Yen, Hsing-I Hsing, and Yen-Hwei Chang, Jpn. J. Appl. Phys., Part 1 **34**, 6149 (1995).
[6] Javier Junquera and Philippe Ghosez, Nature (London) **422**, 506 (2003).
[7] Y. S. Kim, D. H. Kim, J. D. Kim, Y. J. Chang, T. W. Noh, J. H. Kong, K. Char, Y. D. Park, S. D. Bu, J.-G. Yoon, and J.-S. Chung, Appl. Phys. Lett. **86**, 102907 (2005).
[8] M. Anliker, H. R. Brugger, and W. Kanzig, Helv. Phys. Acta **27**, 99 (1954).
[9] R. Böttcher, C. Klimm, D. Michel, H.-C. Semmelhack, G. Völkel, H.-J. Cläsel, and E. Hartmann, Phys. Rev. B **62**, 2085 (2000); E. Erdem, R. Boettcher, H.-J. Glasel, E. Hartmann, G. Klotzsche, and D. Michel, Ferroelectrics **316**, 43 (2005).
[10] M. D. Glinchuk and A. N. Morozovskaya, Phys. Status Solidi B **238**, 81 (2003); M. D. Glinchuk and P. I. Bykov, J. Phys. Condens. Matter **16**, 6779 (2004).
[11] G. Arlt, J. Mater. Sci. **25**, 2655 (1990); Ferroelectrics **104**, 217 (1990).
[12] G. Arlt, D. Hennings, and G. de With, J. Appl. Phys. **58**, 1619 (1985).
[13] Kyoichi Kinoshita and Akihiko Yamaji, J. Appl. Phys. **47**, 371 (1976).
[14] Aziz S. Shaikh, Robert W. Vest, and Geraldine M. Vest, IEEE Trans. Ultrason. Ferroelectr. Freq. Control **36**, 407 (1989).
[15] A. Yu. Emelyanov, N. A. Pertsev, S. Hoffmann-Eifert, U. Böttger, and R. Waser, J. Electroceram. **9**, 5 (2002).
[16] M. H. Frey, Z. Xu, P. Han, and D. A. Payne, Ferroelectrics **206**, 337 (1998).
[17] T. Kanata, T. Yoshikawa, and K. Kubota, Solid State Commun. **62**, 765 (1987).
[18] Weilie Zhong, Peilin Zhang, Yuguo Wang, and Tianling Ren, Ferroelectrics **160**, 55 (1994).
[19] Baorang Li, Xiaohui Wang, Longtu Li, Hui Zhou, Xingtao Liu, Xiuquan Han, Yingchun Zhang, Xiwei Qi, and Xiangyun Deng, Mater. Chem. Phys. **83**, 23 (2004).
[20] Xiangyun Deng, Xiaohui Wang, Hai Wen, Aiguo Kang, Zhilun Gui, and Longtu Li, J. Am. Ceram. Soc. **89**, 1059 (2006).
[21] V. Buscaglia, M. T. Buscagla, M. Viviani, T. Ostapchuk, I. Gregora, J. Petzelt, L. Mitoseriu, P. Nanni, A. Testino, R. Calderone, C. Harnagea, Z. Zhao, and M. Nygren, J. Eur. Ceram. Soc. **25**, 3059 (2005).
[22] M. H. Frey and D. A. Payne, Phys. Rev. B **54**, 3158 (1996).
[23] G. A. Samara, Phys. Rev. **151**, 378 (1966).
[24] T. Ishidate, S. Abe, H. Takahashi, and N. Mori, Phys. Rev. Lett. **78**, 2397 (1997).
[25] W. R. Buessem, L. E. Cross, and A. K. Goswami, J. Am. Ceram. Soc. **49**, 33 (1966).
[26] A. G. Zembilgotov, N. A. Pertsev, and R. Waser, J. Appl. Phys. **97**, 114315 (2005).
[27] A. J. Bell and L. E. Cross, Ferroelectrics **59**, 197 (1984).
[28] Y. L. Li, L. E. Cross, and L. Q. Chen, J. Appl. Phys. **98**, 064101 (2005).
[29] N. A. Pertsev, A. G. Zembilgotov, and A. K. Tagantsev, Phys. Rev. Lett. **80**, 1988 (1998).
[30] W. L. Zhong, Y. G. Wang, P. L. Zhang, and B. D. Qu, Phys. Rev. B **50**, 698 (1994).
[31] B. Jiang and L. A. Bursill, Phys. Rev. B **60**, 9978 (1999).
[32] M. J. Haun, E. Furman, S. J. Jang, H. A. Mckinstry, and L. E. Cross, J. Appl. Phys. **62**, 3331 (1987).
[33] The list of the parameters of $G$ (in SI units, the temperature $T$ in °C) used in the calculations. For $BaTiO_3$: $\alpha_1(T)=4.124\times10^5(T-115)$ Jm/C$^2$; $\alpha_{11}=-2.097\times10^8$ Jm$^5$/C$^4$; $\alpha_{12}=7.974\times10^8$ Jm$^5$/C$^4$; $\alpha_{111}=1.294\times10^9$ Jm$^9$/C$^6$; $\alpha_{112}=-1.950\times10^9$ Jm$^9$/C$^6$; $\alpha_{123}=-2.500\times10^9$ Jm$^9$/C$^6$; $\alpha_{1111}=3.863\times10^{10}$ Jm$^{13}$/C$^8$; $\alpha_{1112}=2.529\times10^{10}$ Jm$^{13}$/C$^8$; $\alpha_{1122}=1.637\times10^{10}$ Jm$^{13}$/C$^8$; $\alpha_{1123}=1.367\times10^{10}$ Jm$^{13}$/C$^8$; $Q_{11}=0.11$ m$^4$/C$^2$; $Q_{12}=-0.043$ m$^4$/C$^2$; $Q_{44}=0.059$ m$^4$/C$^2$; $S_{11}=8.3\times10^{-12}$ m$^2$/N; $S_{12}=-2.5\times10^{-12}$ m$^2$/N; $S_{44}=9.24\times10^{-12}$ m$^2$/N.
[34] George A. Rossetti, Jr., K. R. Udayakumar, Michael J. Haun, and L. Eric Cross, J. Am. Ceram. Soc. **73**, 3334 (1990).
[35] George A. Rossetti, L. Eric Cross, and Keiko Kushida, Appl. Phys. Lett. **59**, 2524 (1991).
[36] Zhe Zhao, Vincenzo Buscaglia, Massimo Viviani, Maria Teresa Buscaglia, Liliana Mitoseriu, Andrea Testino, Mats Nygren, Mats Johnsson, and Paolo Nanni, Phys. Rev. B **70**, 024107 (2004).
[37] G. Catalan, B. Noheda, J. McAneney, L. J. Sinnamon, and J. M. Gregg, Phys. Rev. B **72**, 020102(R) (2005).
[38] Maria Teresa Buscaglia, Massimo Viviani, Vincenzo Buscaglia, Liliana Mitoseriu, Andrea Testino, Paolo Nanni, Zhe Zhao, Mats Nygren, Catalin Harnagea, Daniele Piazza, and Carmen Galassi, Phys. Rev. B **73**, 064114 (2006).
[39] J. L. Zhu *et al.* (unpublished).